On the Reynolds stress and zonal flows in the edge of tokamaks.

M. Vergote, M. Van Schoor, Y. Xu, S. Jachmich

Euratom-Etat Belge' - Associatie 'Euratom-Belgische Staat', Ecole Royale Militaire - Koninklijke Militaire School, Avenue de la Renaissance, Renaissancelaan 30, B-1000 Brussels, Belgium, Partner in the Trilateral Euregio Cluster (TEC).

Introduction

It is well known that turbulence, the major candidate to explain anomalous transport, can be quenched by sheared flows which rip the convective cells apart, thus forming a barrier. The opposite mechanism, i.e. the turbulence generating a macroscopical sheared flow, has been studied as well, both on the theoretical side [1], as on the experimental one [2]. Knowing that the turbulence in the edge of the plasma is quasi-electrostatic, we recently developed a 1D model [3], which calculates the poloidal acceleration profile, due to the flux surface averaged influence of the electrostatic Reynolds stresses, in presence of bulk viscosity and neutrals.

Now we would like to study the link between Reynolds stress and zonal flows (defined by $k_{\theta} << k_r$). Therefore we chose a turbulence model, where the fluctuating velocity of the ions lies in the perpendicular plane. The electrons are considered as an isothermal fluid, providing charge neutrality by flowing along the field line against resistivity. The resulting model is the famous Hasegawa-Wakatani (H.-W.) model [4] in 2D (r, θ) and is based on two independent fluctuating quantities (number density n and electric potential ϕ), which are driven by a background density profile $n_o(r)$. We confront this model with experimentally measured turbulence in CASTOR, and reported in [3].

Theoretical modelling

To the original H.-W. model [4], we added curvature terms representing the effect of the curved and inhomogeneous magnetic field[5], as well as particle diffusion in the electron continuity equation, to increase the stability during the numerical calculations. With the proper non-dimensional definition of the electron density $n' = \frac{n}{n_o}$ and the potential $\phi' = \frac{e\phi}{k_BT}$, we can write our model equations:

$$(\partial_{t'} - [\phi',])\nabla'^{2}_{\perp}\phi' = C_{1}(\phi' - n') + C_{2}\nabla'^{2}_{\perp}(\nabla'^{2}_{\perp}\phi') - \omega_{B}\mathbf{K}'(n')$$
(1)

$$(\partial_{t'} - [\phi',])n' = C_1(\phi' - n') + \partial_{v'}\phi'\partial_{x'}(\ln n_o) + \omega_B \mathbf{K}'(\phi' - n') + C_2 \nabla_{\mid}^{\prime 2} n'$$
(2)

in which the primes denote dimensionless quantities $(x' = x/\rho_i, y' = y/\rho_i, t' = \omega_{ci}t)$ and $[\bullet, \bullet]$ are Poisson brackets. The adiabaticity coefficient of the electron response is abbreviated by

 $C_1 = \frac{kT_e\sigma_z}{e^2\omega_{ri}n_o}k_z^2$ (k_z^2 is determined by the background density gradient through the assumption of maximum growth rate [4]) and the kinematic ion shear viscosity μ is introduced by $C_2 = \frac{\mu}{\omega_{ci}\rho_i^2}$, with ρ_i the Larmor radius, ω_{ci} the ion cyclotron frequency and σ_z the electron conductivity in the parallel direction. The evolution of these dynamical equations is computed locally by a pseudospectral code, for the time being on a rectangular grid x - y with periodic boundary conditions (x representing the minor radial direction r, y tangent to the poloidal direction θ). The curvature depends on the poloidal angle through the operator $\mathbf{K}'(f) = (\sin\theta \partial_{x'} + \cos\theta \partial_{y'})f$, with $\omega_B = \frac{2\rho_i}{R_o}$. The real space between two different grid points is smaller than half a gyro radius: in all calculations we used $\rho_i/2.1$, so that the maximum dimensionless wavenumber is 2.1π in both directions. Wavenumbers in absolute value above 2π are artificially damped by a hyperviscosity in the vorticity equation [6]. The time stepping algorithm is based on a predictor-corrector scheme.

Comparison with experimental data from Castor

To compare with the data taken at Castor and reported in [3], we put 3 "probe pins" in a grid of 33×33 points $(=8\times8 \text{mm} \text{ in real units})$ at the same relative position as the pins of the real probe used in [3](on top of the tokamak, $\theta = \pi/2$, see Fig. 4). We simulated the self consistent generation of turbulence on the basis of equations (1)-(2) and sampled the signals at the same frequency as during the experiment(1 MHz). The coefficients C_1 , C_2 and ω_B are computed according to the edge for the potential and the density (by parameters of Castor ($T_i \approx 20 \text{eV}$, $n_i = 1.5 \times 10^{19} 1/m^3$, simulation and on CASTOR). $\nabla n_i = -7.5 \times 10^{20} 1/m^4$ and $R_o = 0.40m$, a = 0.085m,

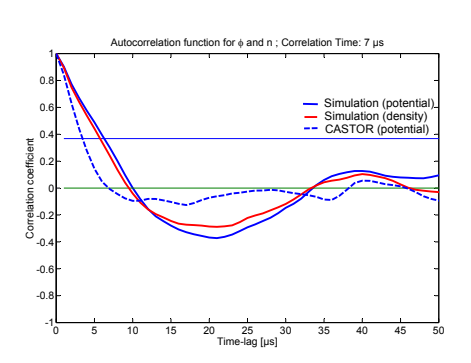


Figure 1: Auto-correlation function

 $B_T = 1T$). The correlation time $\tau \approx 7 \mu s$ (see Fig. 1) confirms the experimental findings [7]. A

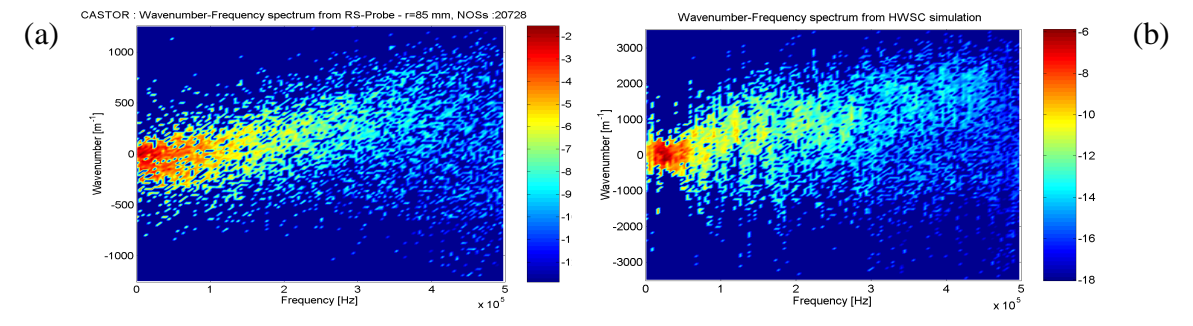


Figure 2: (a) Wavenumber-frequency spectrum $S(k_{\theta}, f)$ from CASTOR (just inside the limiter), and (b) from simulation

more profound cross check of the code can be done by looking at the wavenumber-frequency spectrum shown in Fig. 2, derived from ohmical CASTOR data by the experimental two-point correlation technique, proposed in [8]. The experiment reveals a phase velocity ω/k of the order of 6000m/s (Fig. 2.(a)), somewhat higher than the one derived from simulation (v_{ph} =1200 m/s - Fig. 2(b)).

Now if we look at the fluctuation levels of ϕ and the Reynolds stress (Fig. 3), it is clear that the simulated fluctuation levels are somewhat lower than experimentally observed (factor of 3 for the raw data, one order of magnitude for the Reynolds stress). Nevertheless, the behavior is quite similar.

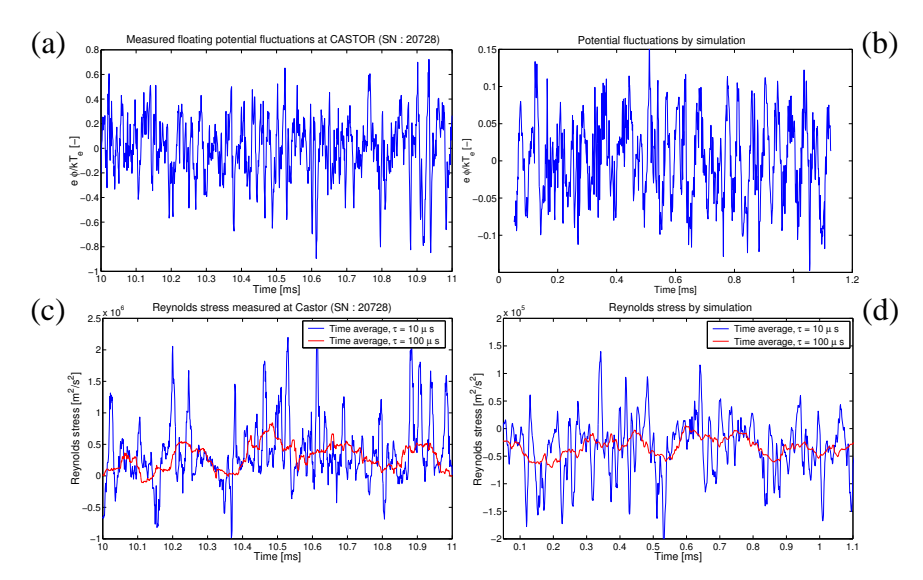


Figure 3: Up: floating potential [dimensionless] at Castor (a) and simulated (b). Bottom: time averaged value (blue: rapid fluctuations with a boxcar window of $\tau = 10\mu s$; red: slow ... $\tau = 100\mu s$) of Reynolds stress at Castor (c) and from simulation (d).

Looking further at the time trace of the potential and density fluctuations starting from a standard k-spectrum (Fig. 5.), we can distinguish several possible states of the turbulence. In our case of interchange turbulence with CASTOR relevant parameters, a simple

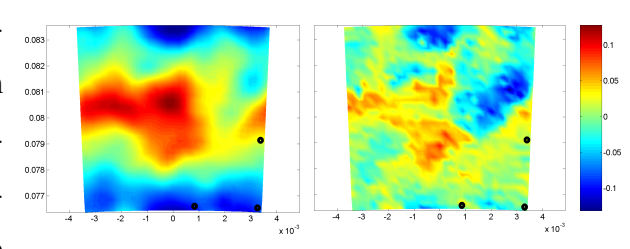


Figure 4: *Snapshot of* ϕ *and* n.

snapshot of the grid (at saturation) reveals that the density and the potential fluctuations are out of phase. A typical cross-correlation coefficient between them is ≈ 0.15 , compared to $\approx 0.2-0.35$ experimentally (depending on minor radius). Moreover, the computations present over the time of simulation periods during which the anomalous transport is reduced (by a factor of 3 to the nominal value, $D_{nom} = -\frac{\langle \widetilde{nv}_r \rangle}{\nabla n} \approx 0.2 m^2/s$). Interestingly, the transitions from

low to strong diffusion seem to be accompanied by more Reynolds stress activity. This means that Reynolds stress is the driving force behind the transition. In the quiet situations the turbulence organises itself in a poloidally elongated structure for what concerns the electric potential, which can be interpreted as a zonal flow $(k_{\theta} < k_r)$. With the restrictions on the grid size, this condition for zonal flow is rather difficult to verify on the wavenumber-spectrum (see peaks A and B on Fig. 5(a)). On the frequency spectrum (Fig. 5(b)) we can distinguish a peak in the spectrum at a frequency of about f = 25 kHz, which could support the indication of a zonal flow.

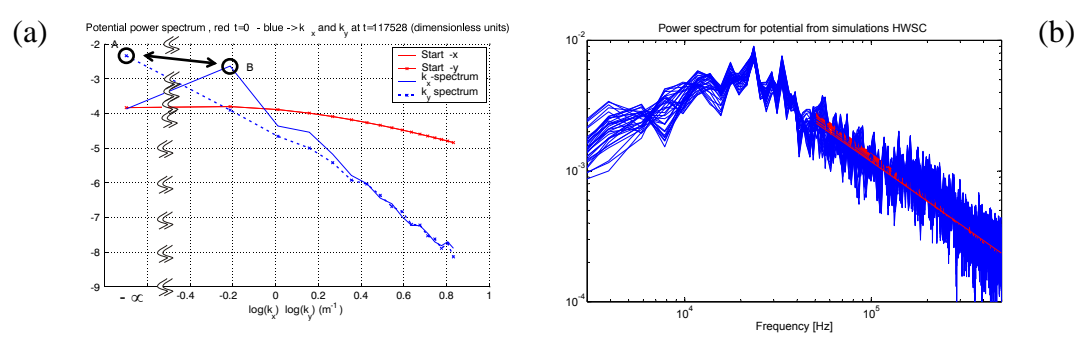


Figure 5: *Instantaneous wavenumber-spectrum for the potential fluctuations (a), and spectrum of the fluctuating floating potential (b) during "zonal flow" situation.*

Conclusion

Our model seems to lead to relevant results with respect to the measurements made at the edge in Castor, on behalf of the level of the fluctuations, which is slightly too low. This model predicts somehow as well the (temporarily) existence of zonal flows in the saturated state of the turbulence, during which the anomalous diffusion is reduced. The role of the Reynolds stress herein needs further investigation.

References

- [1] P.H. Diamond et al. *Physics of Fluids*, B3(7):1626, 1991.
- [2] Y.H. Xu et al. *Physical Review Letters*, 84(17):3867, 2000.
- [3] M. Vergote et al. Czech Journal of Physics, 55:389, 2005.
- [4] Hasegawa and Wakatani. *Physics of Fluids*, 27:611, 1984.
- [5] B. Scott. Plasma Physics and Controlled Fusion, 39:471, 1997.
- [6] S.A. Smith. *Phys. of Plasmas*, 4:978, 1997.
- [7] Martines et al. Plasma Phys and Contr Fusion, 44:351, 2002.
- [8] Ch. P. Ritz et al. Rev. Sci Instrum., 59(8):1739, 1988.